Summer Precipitation Frequency, Intensity, and Diurnal Cycle over China: A Comparison of Satellite Data with Rain Gauge Observations

TIANJUN ZHOU

LASG, Institute of Atmospheric Physics, Chinese Academy of Sciences, Beijing, China

RUCONG YU

LASG, Institute of Atmospheric Physics, Chinese Academy of Sciences, and LaSW, Chinese Academy of Meteorological Sciences, Beijing, China

HAOMING CHEN

LASG, Institute of Atmospheric Physics, Chinese Academy of Sciences, and Graduate School of Chinese Academy of Sciences, Beijing, China

AIGUO DAI

National Center for Atmospheric Research, Boulder, Colorado*

YANG PAN

LASG, Institute of Atmospheric Physics, Chinese Academy of Sciences, and Graduate School of Chinese Academy of Sciences, Beijing, China

(Manuscript received 7 May 2007, in final form 28 December 2007)

ABSTRACT

Hourly or 3-hourly precipitation data from Precipitation Estimation from Remotely Sensed Information using Artificial Neural Networks (PERSIANN) and Tropical Rainfall Measuring Mission (TRMM) 3B42 satellite products and rain gauge records are used to characterize East Asian summer monsoon rainfall, including spatial patterns in June–August (JJA) mean precipitation amount, frequency, and intensity, as well as the diurnal and semidiurnal cycles. The results show that the satellite products are comparable to rain gauge data in revealing the spatial patterns of JJA precipitation amount, frequency, and intensity, with pattern correlation coefficients for five subregions ranging from 0.66 to 0.94. The pattern correlation of rainfall amount is higher than that of frequency and intensity. Relative to PERSIANN, the TRMM product has a better resemblance with rain gauge observations in terms of both the pattern correlation and root-mean-square error. The satellite products overestimate rainfall frequency but underestimate its intensity. The diurnal (24 h) harmonic dominates subdaily variations of precipitation over most of eastern China. A late-afternoon maximum over southeastern and northeastern China and a near-midnight maximum over the eastern periphery of the Tibetan Plateau are seen in the rain gauge data. The diurnal phases of precipitation frequency and intensity are similar to those of rainfall amount in most regions, except for the middle Yangtze River valley. Both frequency and intensity contribute to the diurnal variation of rainfall amount over most of eastern China. The contribution of frequency to the diurnal cycle of rainfall amount is generally overestimated in both satellite products. Both satellite products capture well the nocturnal peak over the eastern periphery of the Tibetan Plateau and the late-afternoon peak in southern and northeastern China. Rain gauge data over the region between the Yangtze and Yellow Rivers show two peaks, with one in the early morning and the other later in the afternoon. The satellite products only capture the major late-afternoon peak.

* The National Center for Atmospheric Research is sponsored by the National Science Foundation.

Corresponding author address: Dr. Tianjun Zhou, LASG, Institute of Atmospheric Physics, Chinese Academy of Sciences, 100029 Beijing, China.
E-mail: zhoutj@lasg.iap.ac.cn

DOI: 10.1175/2008JCLI2028.1

1. Introduction

Large-scale analyses of precipitation have traditionally focused on accumulated amounts or time-averaged mean rates, while other characteristics of precipitation, such as frequency and intensity, have been the foci of only recent studies (e.g., Dai 2001a,b; Trenberth et al. 2003; Dai et al. 2007; DeMott et al. 2007; Sun et al. 2006, 2007). Together with the diurnal cycle, which is large for rainfall over land during the warm season (e.g., Dai 2001b; Dai et al. 2007), these precipitation characteristics significantly modulate soil moisture, runoff, evaporation, and sensible heat flux over land (Qian et al. 2006). They also provide an excellent test bed for validating cumulus and other parameterizations in numerical weather and climate models, which still have large deficiencies in simulating the diurnal timing, frequency, and intensity of precipitation (e.g., Dai et al. 1999; Lin et al. 2000; Yang and Slingo 2001; Betts and Jakob 2002; Dai and Trenberth 2004; Liang et al. 2004; Dai 2006; Demott et al. 2007; Lee et al. 2007).

The diurnal cycle of precipitation, which comes largely from its frequency variations (Dai et al. 1999, 2007), has large spatial and seasonal variations. The dominant feature of the oceanic diurnal cycle is a rainfall maximum in early morning (0400–0600 LST), whereas warm-season precipitation peaks in late afternoon (1500–1900 LST) over most (but not all) land areas (Dai 2001b; Dai et al. 2007). This land–sea contrast is accompanied by a large-scale land–ocean diurnal circulation with rising (sinking) motion in late afternoon over the warm continents (adjacent cool oceans) and the opposite during early morning (Dai and Deser 1999). During the cold season, the diurnal cycle in precipitation is much weaker and tends to peak in the morning over land, while the seasonal changes are relatively small over oceans (Dai 2001b; Dai et al. 2007). Besides the global analyses by Dai and others, there are also many regional studies of the diurnal cycle over the United States (e.g., Wallace 1975; Dai et al. 1999), the coastal and island regions in Asia (e.g., Oki and Musiake, 1994; Yang and Slingo 2001), tropical Americas (Kousky 1980), and West Africa (Shinoda et al. 1999; Pinker et al. 2006). Partly because of a lack of high-resolution data, precipitation frequency, intensity, and their diurnal variations over China have not been well documented. Previous studies of diurnal variations of precipitation over China used data from a limited number of stations, often within a small region, and focused on precipitation amount or mean rates (e.g., Lu 1942; Yeh and Gao 1979; Zhao et al. 2005). A recent analysis on the mean precipitation rate by Yu et al. (2007a) shows that summer precipitation over contiguous China has large diurnal variations with considerable regional features. For example, over southern inland and northeastern China, summer precipitation peaks in late afternoon, while over most of the Tibetan Plateau and its eastern periphery it peaks around midnight. The diurnal phase varies eastward along the Yangtze River valley.

Precipitation data with high spatial and temporal resolution are required for studying the precipitation characteristics over China to resolve the complex coastlines and topography. As shown in Fig. 1, the terrain over central China varies from the hills and plains in the east to the Sichuan Basin in the center and the Tibetan Plateau in the west. Over southeastern China, the terrain is dominated by complex coastlines. To help resolve the spatial distribution of precipitation over this complex terrain, here we use hourly rain gauge measurements from 626 stations supplemented with hourly or 3-hourly, 0.25°-gridded rainfall data from satellite observations. The satellite products we used include the Precipitation Estimation from Remotely Sensed Information using Artificial Neural Networks (PERSIANN; Sorooshian et al. 2000) and Tropical Rainfall Measuring Mission (TRMM) 3B42 datasets (Huffman et al. 2007). Because precipitation over most of China occurs mainly from June to August (Tao and Chen 1987) and the diurnal cycle is strongest during the summer (Dai et al. 2007), we will focus on the June–August (JJA). This is also the eastern Asian summer monsoon season (Zhou and Li 2002; Zhou and Yu 2005). We want to address the following questions: 1) What are the spatial structures of summer monsoon precipitation characteristics over eastern China, including not only the precipitation amount but also its frequency and intensity, and their diurnal cycles? 2) Are the satellite data useful for studying precipitation frequency, intensity, and diurnal cycle over contiguous China?

Our results show that the diurnal harmonic dominates variations of precipitation over most of eastern China. A late-afternoon maximum over southeastern and northeastern China and a near-midnight maximum over the eastern periphery of the Tibetan Plateau are seen in the amount, frequency, and intensity measured by rain gauges. Both the PERSIANN and TRMM 3B42 satellite products capture the diurnal phase of precipitation amount, except with bias in amplitude. The satellite products overestimate frequency but underestimate intensity of rainfall. The quality of satellite products in the area between the Yangtze and Yellow Rivers is poor; the observed secondary early morning peak is missing in satellite measurements.

The paper is organized as follows: section 2 describes the datasets and analysis method; a comparison of the

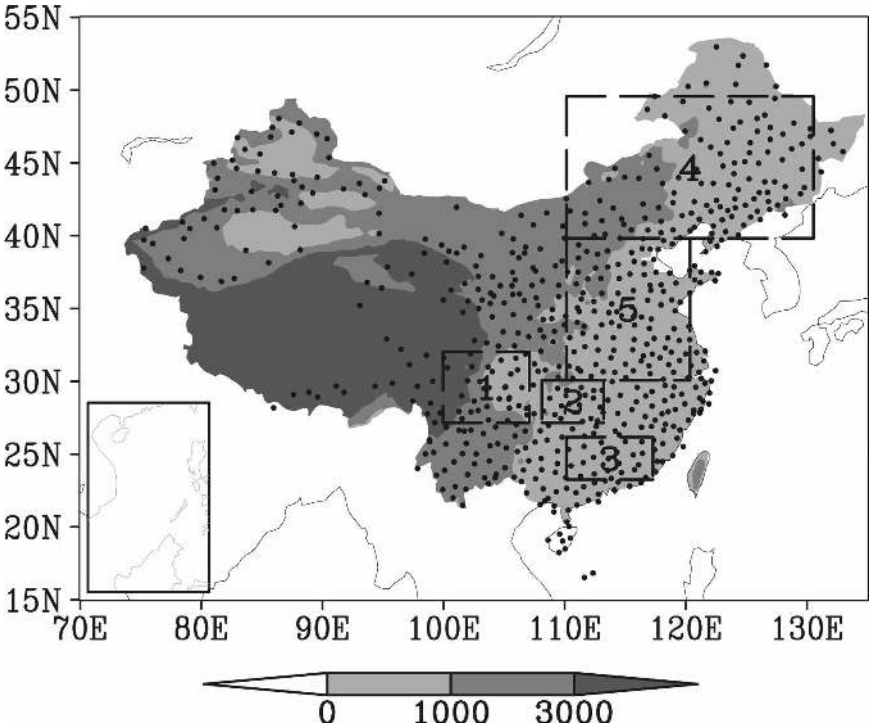

FIG. 1. Surface elevation (shaded, m) over China, together with locations of the 626 rain gauge stations (black dots) used in this study. Five subregions are outlined for regional averaging.

monthly mean precipitation amount, frequency, and intensity between the satellite data and rain gauge measurements is presented in section 3. The diurnal (24 h) cycle of summer precipitation amount, frequency, and intensity over eastern China is discussed in section 4. Section 5 describes the mean semidiurnal (12 h) cycle of precipitation amount, frequency, and intensity. A summary and discussion are given in section 6.

2. Data and analysis method

The surface precipitation dataset used in this study was obtained from the National Meteorological Information Center of the China Meteorological Administration. It consists of quality-controlled (Yu et al. 2007a) hourly rain gauge records from 2000–04 at 626 stations. Most of the stations are located in central and eastern China (Fig. 1) with only sparse coverage over western China, especially the western part of the Tibetan Plateau. To facilitate analysis, the original station data were interpolated onto a 0.5° latitude × 0.5° longitude grid by averaging the station data with weights proportional to the inverse of the squared distance between the center of the grid box and the stations within a radius of 1°. If the distance is less than 0.1°, the weight number of the station data will be 1 (Chang 2003).

The first satellite product used in this study is the PERSIANN dataset (Hsu et al. 1999; Sorooshian et al. 2000). Here we used the PERSIANN hourly precipitation data from 2000–04 on a 0.25° grid (60°S–60°N). In the PERSIANN system, a neural network trained by precipitation from TRMM Microwave Imager (TMI) and other microwave measurements (Hsu et al. 1997, 1999) was used to estimate 30-min precipitation rates from infrared (IR) and visible imagery from geostationary satellites.

In addition to the PERSIANN data, the TRMM 3B42 (3 hourly, 0.25°) precipitation data from 2000–04 (Huffman et al. 2007) are also used. This product was derived by using an optimal combination of microwave rain estimates from TRMM, Special Sensor Microwave Imager (SSM/I), Advanced Microwave Scanning Radiometer (AMSR), and Advanced Microwave Sounding Unit (AMSU) to adjust IR estimates from geostationary IR observations. The 3B42 estimates are scaled to match the monthly rain gauge observations. To improve the comparability, both the PERSIANN and TRMM data were remapped onto the same 0.5° grid as the rain gauge data.

At each grid box and for each hour, the JJA averages of precipitation frequency [defined as the percentage of all hours during JJA having measurable precipitation,

defined here as >0.02 mm h^{-1} (or 0.5 mm day^{-1}) for the gridded precipitation from rain gauge and satellite observations], intensity (the mean rates averaged over the precipitating hours), and amount (the accumulated precipitation amount during JJA, which is the product of the frequency, intensity, and number of days for JJA) were computed for each year. The multiyear (2000–04) mean states of JJA frequency and intensity were derived by averaging the hourly or 3-hourly frequency and intensity. The JJA mean hourly data were averaged over the years to derive a composite diurnal cycle of these precipitation quantities from which the diurnal and semidiurnal harmonics were estimated. We focus our analysis on the amount, frequency, and intensity of measurable precipitation. The definition of measurable precipitation (a function of resolution) varies among different studies. Dai et al. (1999) used a threshold of 0.1 mm h^{-1} (i.e., 2.4 mm day^{-1}) for the gridded U.S. hourly precipitation, while Dai (2006) and Dai et al. (2007) used a threshold of 1.0 mm day^{-1} for daily precipitation frequency over the globe. The precision of rain gauge measurements in China is 0.1 mm day^{-1} (China Meteorological Administration 2003). Because the mean frequency and intensity are dependent on the threshold, we have performed some sensitivity tests that showed our conclusions to be insensitive to this choice of threshold. For example, employing a threshold of 0.04 and 0.08 mm h^{-1}, respectively, revealed similar patterns of frequency, intensity, and diurnal cycle. A higher threshold is associated with less frequency and stronger intensity but no significant change of diurnal cycle (figures not shown here). A threshold much larger than 0.02 mm h^{-1} greatly reduces the sample size. Here, only the results using a threshold of 0.02 mm h^{-1} are presented.

To characterize the diurnal cycle of precipitation, the amplitudes and phases of the diurnal (24h, S_1) and semidiurnal (12h, S_2) harmonics of precipitation amount, frequency, and intensity are estimated by using least squares fitting (Dai 2001b). This amplitude and the preferred time of maximum is shown using vector plots in a fashion similar to those of Dai et al. (1999) and Liang et al. (2004).

3. Mean precipitation amount, frequency, and intensity

The PERSIANN and TRMM satellite products have been applied to study tropical precipitation and convection and to evaluate climate models (e.g., Adler et al. 2000; Bowman 2005; Dai 2006; Yang and Smith 2006); however, their ability to represent precipitation frequency, intensity, and amount over East Asia has not been verified by independent surface observations. Figure 2 compares 2000–04 mean JJA precipitation amount, frequency, and intensity from rain gauges and the two satellite products. The corresponding pattern correlation coefficients and root-mean-square error (RMSE) between the rain gauge and satellite measurements are listed in Table 1. Typical summer monsoon rainband is located to the east of 100°E and stretches from the southwest to the northeast. Rainfall centers are seen to the eastern periphery of the Tibetan Plateau around 30°N, 102.5°E. Several weak rainfall centers along the middle to lower reaches of the Yangtze River valley are also observed by rain gauges (Fig. 2a). The satellite data show large-scale patterns that resemble rain gauge observations, although the PERSIANN product generally underestimates the JJA precipitation amount, and the rain belt extends west of 100°E in both satellite products. The pattern correlation coefficient with the rain gauge observation is 0.79 for PERSIANN data and 0.94 for TRMM data. The RMSE of TRMM is less than that of PERSIANN, with 1.01 mm day^{-1} versus 1.62 mm day^{-1} (Table 1). The TRMM precipitation has a better spatial resemblance; for example, the rainfall center located between the Yangtze and Yellow Rivers is seen in the TRMM data but absent in the PERSIANN product. In addition, the PERSIANN product shows a strong precipitation center over the plateau areas (27.5°N, 92.5°E), while the TRMM product does not. Since rain gauges are sparse over this area, this feature requires further investigation.

The broad features of the frequency maps (Figs. 2d–f) are comparable among three datasets, and they are similar to those of mean precipitation amount (Figs. 2a–c). The frequency patterns derived from both satellite products are reasonably realistic, with a spatial correlation coefficient with rain gauge data of 0.71 for PERSIANN and 0.77 for TRMM. The RMSEs for TRMM and PERSIANN are 6.84% and 7.63%, respectively (Table 1). The satellite-derived frequency is generally higher than that from rain gauge measurements over most of eastern China. For example, the rain gauge data show 10%–16% of the hours with precipitation exceeding 0.02 mm h^{-1} over the regions between the Yangtze and Yellow Rivers, while the satellite products show 16%–24%. The precipitation frequency in rain gauge data is around 8%–10% over most of northeast China, while it is around 12%–18% for PERSIANN and 8%–16% for TRMM. Precipitation events are rare over most of northwest China (2%–8% of the time), except for the most northwestern area where the PERSIANN and TRMM data show a local

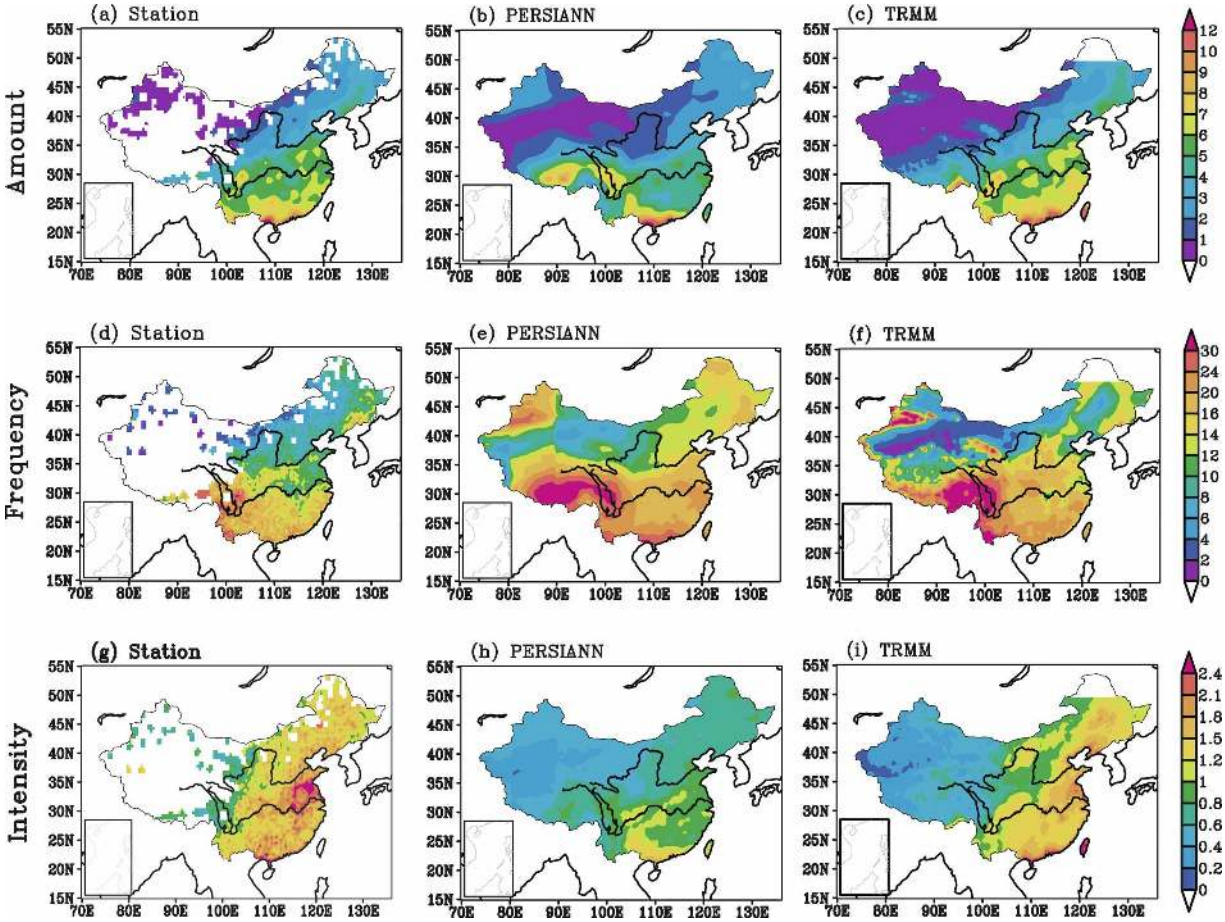

FIG. 2. Spatial distributions of the 2000–04 mean summer (June–August) (a),(b),(c) precipitation amount (mm day^{-1}); (d),(e),(f) frequency (%); and (g),(h),(i) intensity (mm h^{-1}) from (a),(d),(g) rain gauges; (b),(e),(h) PERSIANN; and (c),(f),(i) TRMM3 3B42 products. The Yellow River (north) and Yangtze River (south) are outlined by the black lines.

maximum of 16%–24%. South China has the highest frequency of 14%–24% in the surface observations, whereas the satellite products show a frequency of 18%–24%. The two satellite products show a maximum frequency of 20%–30% over the southeastern Tibetan Plateau (30°N, 102.5°E), which is not evident in the rain gauge data (Figs. 2d–f). The frequency values from the rain gauge measurements are comparable to those of nondrizzle precipitation frequency derived from 3-hourly weather reports (see Fig. 4 in Dai 2001a).

The rain gauge data (Fig. 2g) show a maximum intensity of 1.8–2.4 mm h^{-1} between the lower reaches of the Yangtze and Yellow Rivers, while the intensity is around 1.3–1.9 mm h^{-1} over southeast China and 1.0–1.7 mm day^{-1} over most of northeast China. The intensity is much lower (0.6–1.0 mm day^{-1}) over western China (west of ~100°E). Although these general patterns are reproduced, both satellite products, especially the PERSIANN data, underestimate the intensity, for example, over northeastern China for PERSIANN and western China for TRMM (Figs. 2h,i). The pattern correlation with the rain gauge measurements is 0.67 (0.76) for the PERSIANN (TRMM) product.

We further divide eastern China into five subregions, labeled as follows: Reg1 is the upper reaches of the Yangtze River valley (100°–107°E, 27°–32°N), Reg2 is the middle reaches of the Yangtze River valley (108°–113°E, 27°–30°N), Reg3 is southern China (110°–117°E, 23°–26°N), Reg4 is northeastern China (110°–130°E, 40°–50°N), and Reg5 is Huai River valley (110°–120°E, 30°–40°N), which is the region between the Yangtze and Yellow Rivers. These regions are outlined in Fig. 1 by dashed rectangles. According to the statistics listed in Table 1, the quality of the TRMM product is superior to that of PERSIANN in measuring the precipitation amount over all five subregions; this is supported by both the pattern correlation coefficient and RMSE. The qualities of two satellite products are generally

TABLE 1. Pattern correlation coefficients and RMSE (units: mm day^{-1} for amount, % for frequency, and mm h^{-1} for intensity) between the observed and satellite-derived rainfall amount, frequency, and intensity shown in Fig. 2.

		Pattern correlation		RMSE	
Region	Variable	PERSIANN	TRMM	PERSIANN	TRMM
China	Amount	0.79	0.94	1.62	1.01
	Frequency	0.71	0.77	7.63	6.84
	Intensity	0.66	0.76	0.77	0.45
Reg1	Amount	0.36	0.82	1.39	0.88
	Frequency	0.68	0.58	6.19	7.76
	Intensity	0.29	0.62	0.40	0.31
Reg2	Amount	0.51	0.73	1.08	0.56
	Frequency	0.02	0.28	4.46	3.79
	Intensity	0.19	−0.01	0.62	0.34
Reg3	Amount	0.67	0.82	1.82	1.1
	Frequency	0.55	0.25	5.26	4.67
	Intensity	0.24	0.36	0.78	0.39
Reg4	Amount	0.77	0.95	0.9	0.5
	Frequency	0.81	0.71	5.63	3.09
	Intensity	0.31	0.48	0.77	0.36
Reg5	Amount	0.86	0.91	1.22	0.7
	Frequency	0.50	0.64	6.59	5.13
	Intensity	0.65	0.73	1.04	0.52

poor over Reg2 in measuring the spatial patterns of rainfall frequency and intensity (Table 1).

4. Diurnal cycle of precipitation amount, frequency, and intensity

Figures 3–5 compare the 2000–04 composite diurnal cycles of JJA precipitation amount, frequency, and intensity, respectively, from rain gauges, PERSIANN, and TRMM averaged (at each LST hour) over five subregions of the East Asian summer monsoon (Fig. 1). Large diurnal variations are seen for all five regions, as shown in the mean precipitation rate by Yu et al. (2007a). For example, the rain gauge data show a large peak around 0200 LST at Reg1 and a strong peak around 1700 LST over Reg3 and Reg4. These features are clear in the amount, frequency, and intensity diurnal cycles. Summer precipitation over Reg2 and Reg5 has two diurnal peaks in the amount, frequency, and intensity: one in the early morning (0500 LST) and another in the late afternoon (1600 LST). In general, the satellite data show comparable diurnal variations over Reg1, Reg3, and Reg4. The diurnal phase of intensity in satellite products lags that of rain gauge measurements by several hours over northeastern China. Over Reg2, the early morning peak is stronger than the late afternoon peak in rain gauge data, but the satellite products show the opposite for amount (Fig. 3b) and no morning peaks for frequency (Fig. 4b); both satellite products show a morning peak of intensity, as in the rain gauge data (Fig. 5b). For Reg5, both the PERSIANN and TRMM data show only one peak around 1700 LST in the amount (Fig. 3e), frequency (Fig. 4e), and intensity (Fig. 5e).

To make quantitative estimates on how well the satellite products do in revealing the diurnal cycle of precipitation, correlation and bias analyses are carried out with the curves shown in Figs. 3–5. The statistics are listed in Table 2. The correlations for rainfall amount are generally high (ranging from 0.60 to 0.92), except for Reg2 and Reg5. The low correlation for Reg5 (0.44 for PERSIANN and 0.20 for TRMM) is due to the failure of satellite products in measuring the early morning peak (Fig. 3e), while that for Reg2 (0.33 for PERSIANN and 0.55 for TRMM) is due to the deficiency of satellite products in measuring the major morning peak and minor afternoon peak (Fig. 3b). For the diurnal cycle of rainfall frequency, in addition to the bias of satellite products over Reg2 and Reg5, the correlation of TRMM product over Reg1 is also poor, as already evidenced in Fig. 4a. The correlation of rainfall intensity is generally better than that of frequency, except for the PERSIANN product over Reg4. The bias of the PERSIANN product in measuring daily mean value is generally larger than that of TRMM.

In addition to the diurnal phase, the amplitude of diurnal cycle measured by satellite products should also be assessed. The satellite products show comparable diurnal amplitudes of rainfall amount as those of the rain gauge data over most regions (Fig. 3). However, this does not guarantee good measurements of diurnal amplitude for rainfall frequency and intensity. The

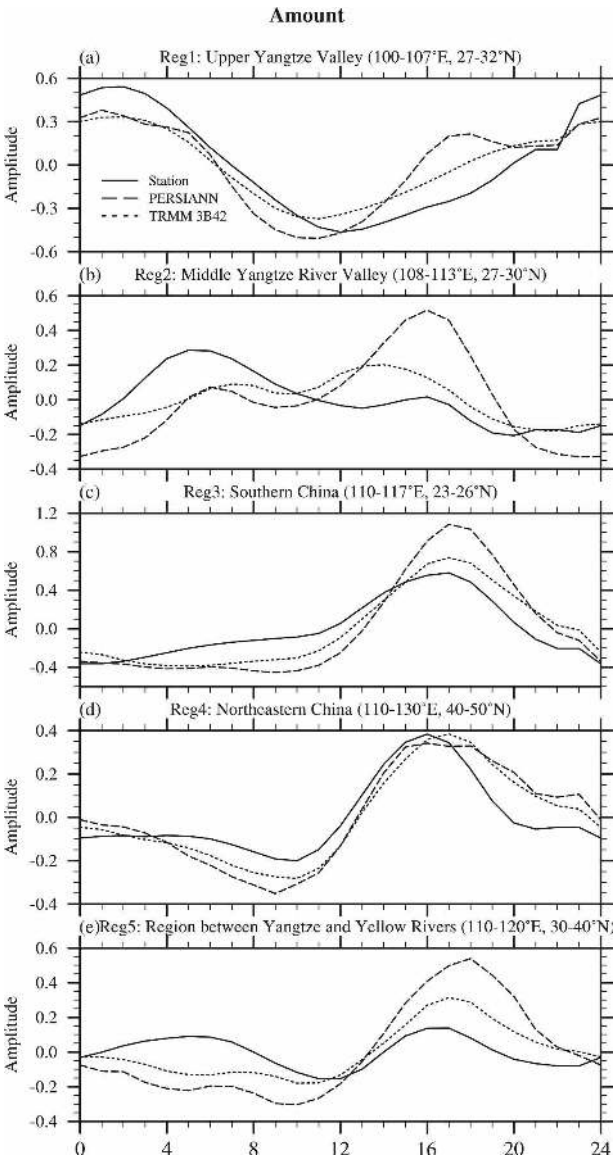

FIG. 3. Mean diurnal cycle of JJA precipitation amount (normalized by the daily mean) averaged over the five selected regions outlined in Fig. 1 from rain gauge measurements (solid line) and two satellite products (dashed: PERSIANN; dotted: TRMM). The unit of x axis is LST in hours.

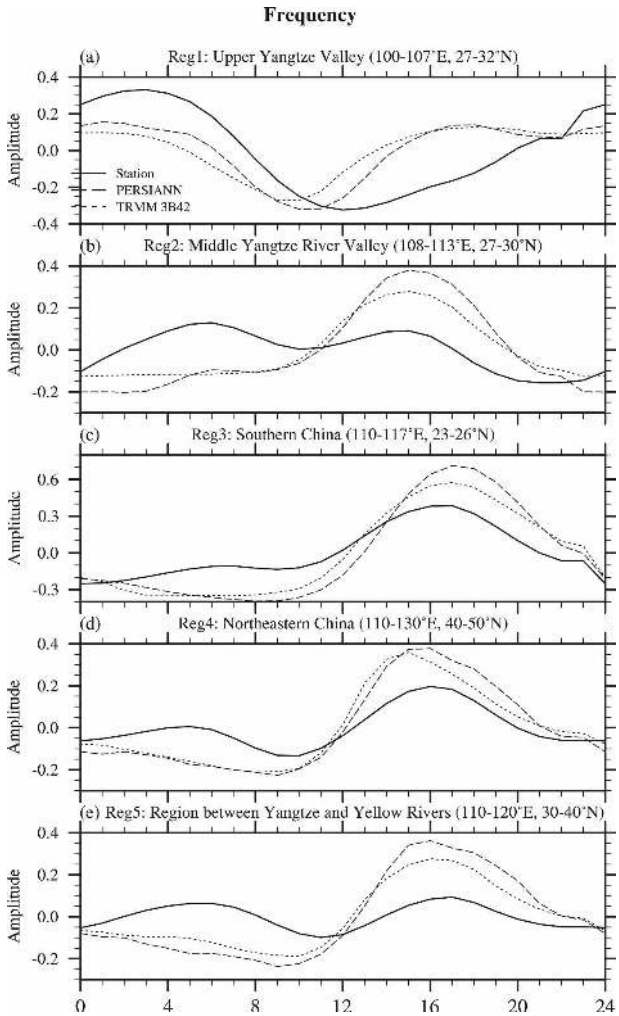

FIG. 4. Same as Fig. 3, but for precipitation frequency.

most prominent feature of Fig. 4 is the overestimation of diurnal amplitude of rainfall frequency in satellite products. The satellite products and rain gauge data show comparable amplitude of rainfall intensity in Reg1 and Reg4 (Fig. 5). The amplitude of rainfall intensity measured by PERSIANN is higher than that of TRMM in Reg3 and Reg5 (Fig. 5).

The correspondence of normalized amplitude of rainfall diurnal cycles derived from the rain gauge and satellite products over different regions are summarized in Table 3. The amplitudes of rainfall amount derived from satellite and rain gauges are comparable, except for Reg3 and Reg5, where both satellite products overestimate the amplitude. The amplitudes of frequency derived from satellite are generally stronger than those of rain gauges, except for Reg1. The amplitude of intensity measured by satellite is stronger than that of rain gauge in Reg2 and Reg5. The daily mean values of frequency and intensity (Table 3) also suggest that the frequency (intensity) of satellite products is generally higher (weaker) than that of rain gauges. Hence, it rains too frequently but too weak in the satellite products. The TRMM data are relatively better than the PERSIANN data in estimating the intensity, as evidenced in both the normalized amplitudes and daily mean values shown in Table 3.

The correspondence of rainfall diurnal phase derived from rain gauge and satellite products over different regions is summarized in Table 4. Overall, the diurnal

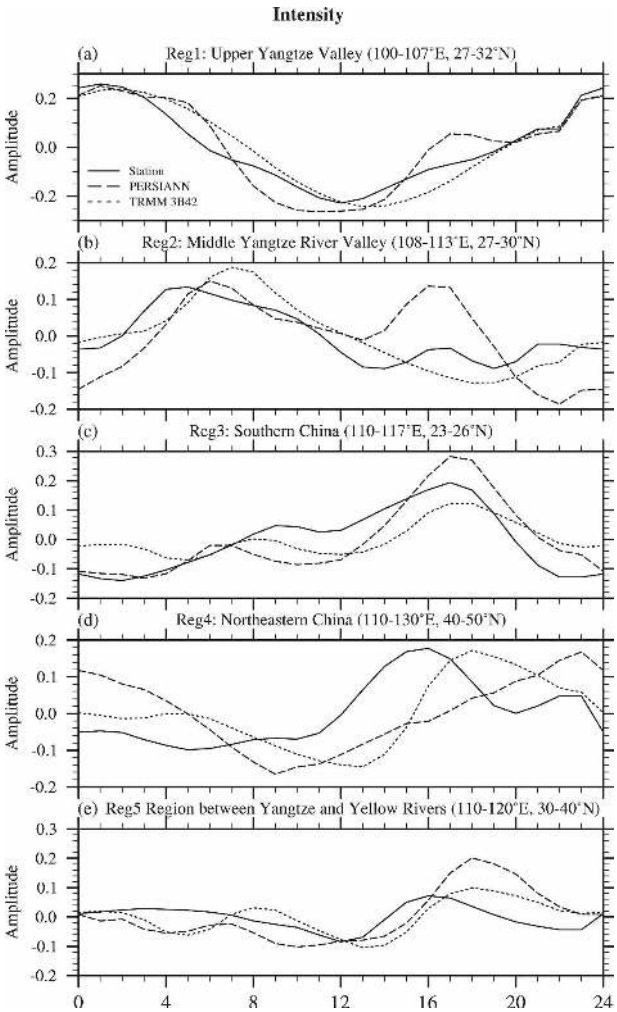

FIG. 5. Same as Fig. 3, but for precipitation intensity.

phases of frequency and intensity are similar to that of precipitation amount, except for Reg2 in rain gauge data. Similar phase relations are seen in both satellite products. Note that the rainfall amount, frequency, and intensity derived from satellites all show a late afternoon major peak over the regions between the Yangtze and Yellow Rivers, although the observed secondary early morning peak is completely missing in the satellite products.

Above analyses suggest that the diurnal cycle of rainfall amount is influenced by both frequency and intensity. To compare the relative contributions of frequency and intensity to the diurnal cycle of rainfall amount, we estimate the percentage variance of diurnal cycle of rainfall amount explained by frequency and intensity. The percentage variance was calculated as the square of correlation coefficient between the diurnal cycles of amount and frequency (intensity). A summary of statistics is presented in Table 4. In observation, the frequency and intensity account for a comparable percentage of the diurnal variation in the precipitation amount over Reg1 and Reg2. The contribution of frequency is slightly higher than that of intensity over the other three subregions. In the satellite products, however, the fractional variance accounted for by frequency is generally larger than that of intensity over nearly all subregions, except for Reg1, suggesting that the contribution of frequency to the diurnal cycle of rainfall amount is overestimated in the satellite products. For example, the variance explained by frequency (83.4%) is far larger than intensity (28.6%) in Reg4 in PERSIANN data. The variances accounted by frequency are 33.3–48.2% higher than that of intensity in Reg2–5 in TRMM data.

Above analyses mainly focus on five subregions. To get a complete picture of contiguous China, Fig. 6 compares the spatial distributions of amplitudes and phases of the diurnal (24 h, S_1) harmonics of multiyear mean JJA precipitation amount, frequency, and intensity from rain gauges and PERSIANN and TRMM products. The direction in which an arrow points denotes the local time at which the maximum amplitude occurs, as indicated by the phase lock in the top left panel (south = 0000, west = 0600, north = 1200, and east = 1800 LST). For example, a vector pointing eastward means that the maximum amplitude occurs at 1800 LST. The S_1 patterns of satellite precipitation amount are in broad agreement with rain gauge measurements (Figs. 6a–c). For example, over southeastern and northeastern China, all three datasets show late-afternoon maxima; over the eastern periphery of the Tibetan Plateau, all three datasets reveal midnight maxima. No coherent arrow pattern is observed over the regions between the Yangtze and Yellow Rivers. As discussed above, this is due to the existence of two comparable peaks, with one in the early morning and the other in the late afternoon (Figs. 3–5). Note that the significance of diurnal cycle over this area expressed by the amplitude is relatively weaker than that in southern China. The diurnal amplitudes from three datasets are comparable over southeastern and northern China.

Over regions with large diurnal cycles in precipitation amount, such as southeastern and northeastern China and the eastern periphery of the Tibetan Plateau (Figs. 6a–c), the frequency also shows large diurnal amplitudes (Figs. 6d–f). Comparing the diurnal cycles between precipitation amount (Figs. 6a–c) and precipitation frequency (Figs. 6d–f) reveals a close resemblance, indicating that the diurnal variation of precipitation amount arises mostly from their frequency, especially

TABLE 2. Correlation coefficients between the diurnal cycles of precipitation derived from rain gauge observations and satellite products shown in Figs. 3–5. Also shown is the bias of daily mean values derived from satellite products relative to rain gauge measurement (units: mm h^{-1} for amount, % for frequency, and mm h^{-1} for intensity).

		Temporal correlation		Bias of daily mean	
Region	Variable	PERSIANN	TRMM	PERSIANN	TRMM
Reg1	Amount	0.74	0.60	0.016	0.025
	Frequency	0.54	−0.23	4.8	5.3
	Intensity	0.89	0.92	−0.23	−0.13
Reg2	Amount	0.33	0.55	−0.038	0.018
	Frequency	0.38	0.26	3.8	2.7
	Intensity	0.43	0.74	−0.57	−0.13
Reg3	Amount	0.92	0.82	−0.058	0.026
	Frequency	0.93	0.81	4.6	3.4
	Intensity	0.81	0.72	−0.71	−0.19
Reg4	Amount	0.84	0.73	−0.019	0.014
	Frequency	0.86	0.30	5.5	2.1
	Intensity	0.17	0.86	−0.70	−0.15
Reg5	Amount	0.44	0.2	−0.041	0.012
	Frequency	0.41	−0.11	6.0	4.5
	Intensity	0.40	0.80	−0.96	−0.44

in the satellite products. The diurnal patterns of frequency derived from satellite products (Figs. 6e–f) are in agreement with rain gauges (Fig. 6d) over regions such as southeastern and northeastern China and the eastern periphery of the Tibetan Plateau. The diurnal amplitudes of satellite products are, however, larger than those of surface observations.

Considerable diurnal variations are also seen in the intensity (Figs. 6g–i). However, the intensity has smaller amplitudes than the amount and frequency do, which is consistent with Figs. 3–5, Table 3, and Dai et al. (1999) over the U.S. domain. The coherent shape of phase distribution for intensity is less obvious as for frequency. Over the eastern periphery of the Tibetan Plateau, the diurnal phase for both intensity and frequency is similar to that of precipitation amount. However, the diurnal phase of intensity often differs from that of frequency over the sites having weak diurnal amplitudes. For the reliability of the satellite products, over the eastern periphery of the Tibetan Plateau and southern China, the diurnal intensity pattern from satellite products is in agreement with rain gauges (Figs. 6g–i). However, the consistency is not as good as the frequency over most areas. The spatially coherent pattern is more obvious in satellite products.

Besides JJA, we have also examined the spatial structures of the precipitation diurnal cycle for other seasons (figures not shown). The main rainband is located to the south of 35°N during December–February. An early morning peak is seen in South China. The diurnal

TABLE 3. The amplitude (% of daily mean) of rainfall diurnal cycle and the corresponding daily mean values (units: mm day^{-1} for amount, % for frequency, and mm h^{-1} for intensity) derived from rain gauge measurements and satellite products over different regions. Here, Ampl = Amplitude, S = Station, P = PERSIANN, and T = TRMM 3B42. Bold numbers indicate that the amplitude of the satellite measurement is larger than that of the rain gauge measurement.

		Amount			Frequency			Intensity		
Regions		S	P	T	S	P	T	S	P	T
Reg1	Ampl.	57	45	36	34	18	13	30	28	25
	Daily mean	5.3	**5.7**	**5.9**	19.2	**24**	**24.6**	1.16	0.93	1.0
Reg2	Ampl.	32	**57**	23	15	**40**	**30**	15	**20**	**22**
	Daily mean	5.5	4.5	**5.8**	14.7	**18.5**	**17.2**	1.56	1.0	1.41
Reg3	Ampl.	64	**115**	**86**	41	**73**	**64**	21	**31**	15
	Daily mean	7.0	5.6	**7.8**	16.7	**21.3**	**20.2**	1.72	1.02	1.57
Reg4	Ampl.	42	41	**45**	21	**42**	**41**	19	18	19
	Daily mean	2.8	2.4	**3.1**	8.2	**13.7**	**10.3**	1.39	0.69	1.24
Reg5	Ampl.	15	**59**	**38**	11	**40**	**41**	9	**23**	**11**
	Daily mean	4.3	3.3	**4.7**	10.1	**16.1**	**14.5**	1.77	0.81	1.36

TABLE 4. The phase of rainfall diurnal cycle derived from rain gauge measurements and satellite products over different regions, as well as the percentage variance of the precipitation amount diurnal variation accounted for by frequency (intensity). Here, Phs = Phase (LST), Var = Variance (%) of the diurnal cycle of precipitation amount explained by frequency and intensity, A = Amount, F = Frequency, and I = Intensity. Bold numbers indicate the larger contribution. Only the phase of major peak is shown.

		Station			PERSIANN			TRMM 3B42		
Regions		A	F	I	A	F	I	A	F	I
Reg1	Phs (LST)	2	2	2	3	2	2	2	2	2
	Var (%)		**95.0**	94.5		90.3	**93.3**		49.0	**80.2**
Reg2	Phs (LST)	7	17	14	7	15	15	6	7	8
	Var (%)		**71.5**	71.0		**83.6**	60.8		**48.3**	9.5
Reg3	Phs (LST)	18	17	17	17	16	17	18	17	17
	Var (%)		**96.3**	85.2		**97.1**	90.2		**96.7**	60.5
Reg4	Phs (LST)	16	17	17	17	15	14	17	23	17
	Var (%)		**91.0**	84.8		**83.4**	28.6		**74.0**	40.7
Reg5	Phs (LST)	17	18	17	17	16	17	17	19	17
	Var (%)		**89.0**	80.1		**89.6**	73.8		**79.1**	30.9

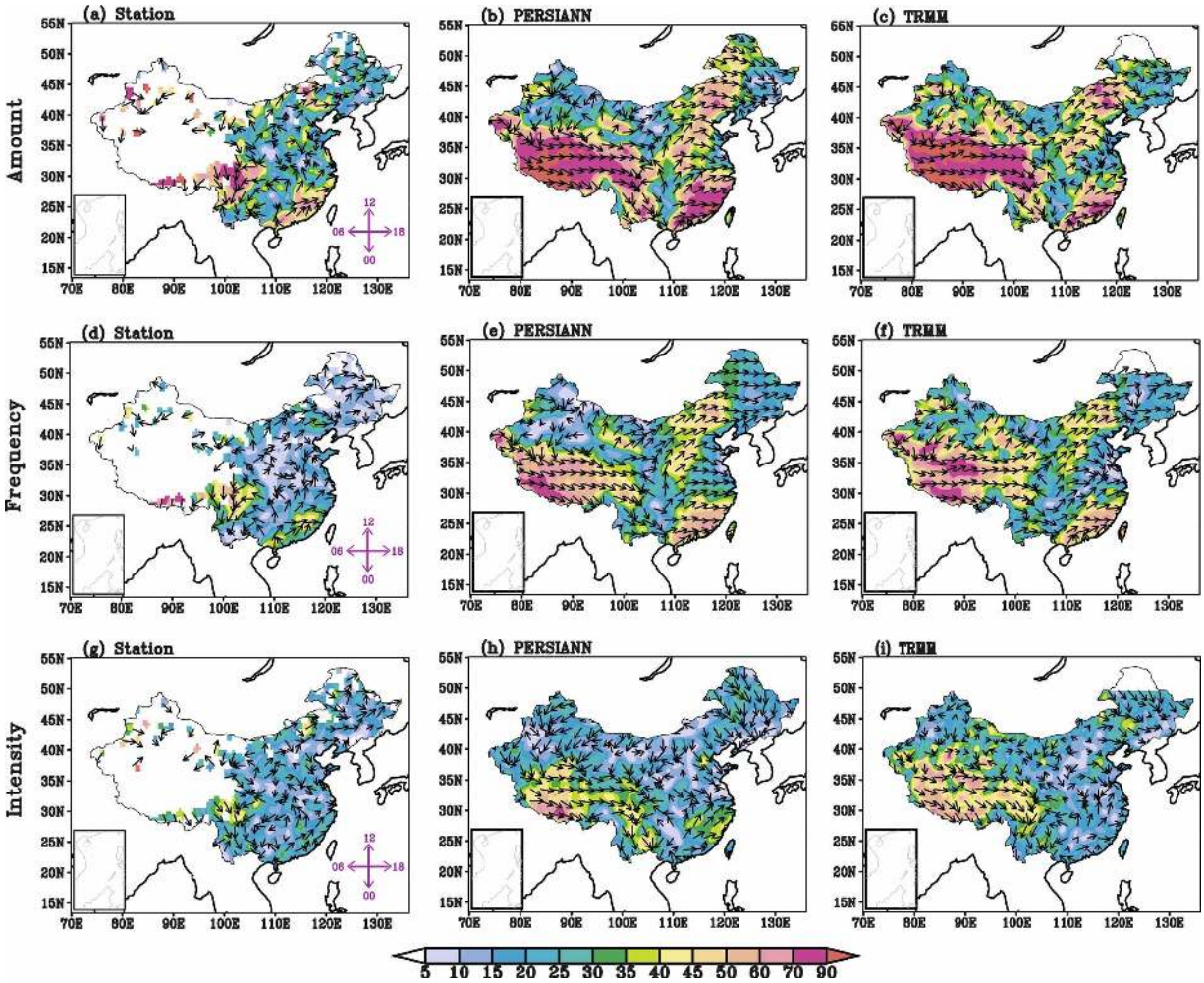

FIG. 6. Spatial distributions of the amplitude (colors) and phase (arrows; LST, see phase clock) of the diurnal (24 h, S_1) harmonics of the 2000–04 mean JJA (a), (b), (c) precipitation amount; (d), (e), (f) frequency; and (g), (h), (i) intensity from (a), (d), (g) rain gauges; (b), (e), (h) PRESIANN; and (c), (f), (i) the TRMM product. The diurnal harmonics were estimated by using least squares fitting. The amplitude was normalized by the daily mean.

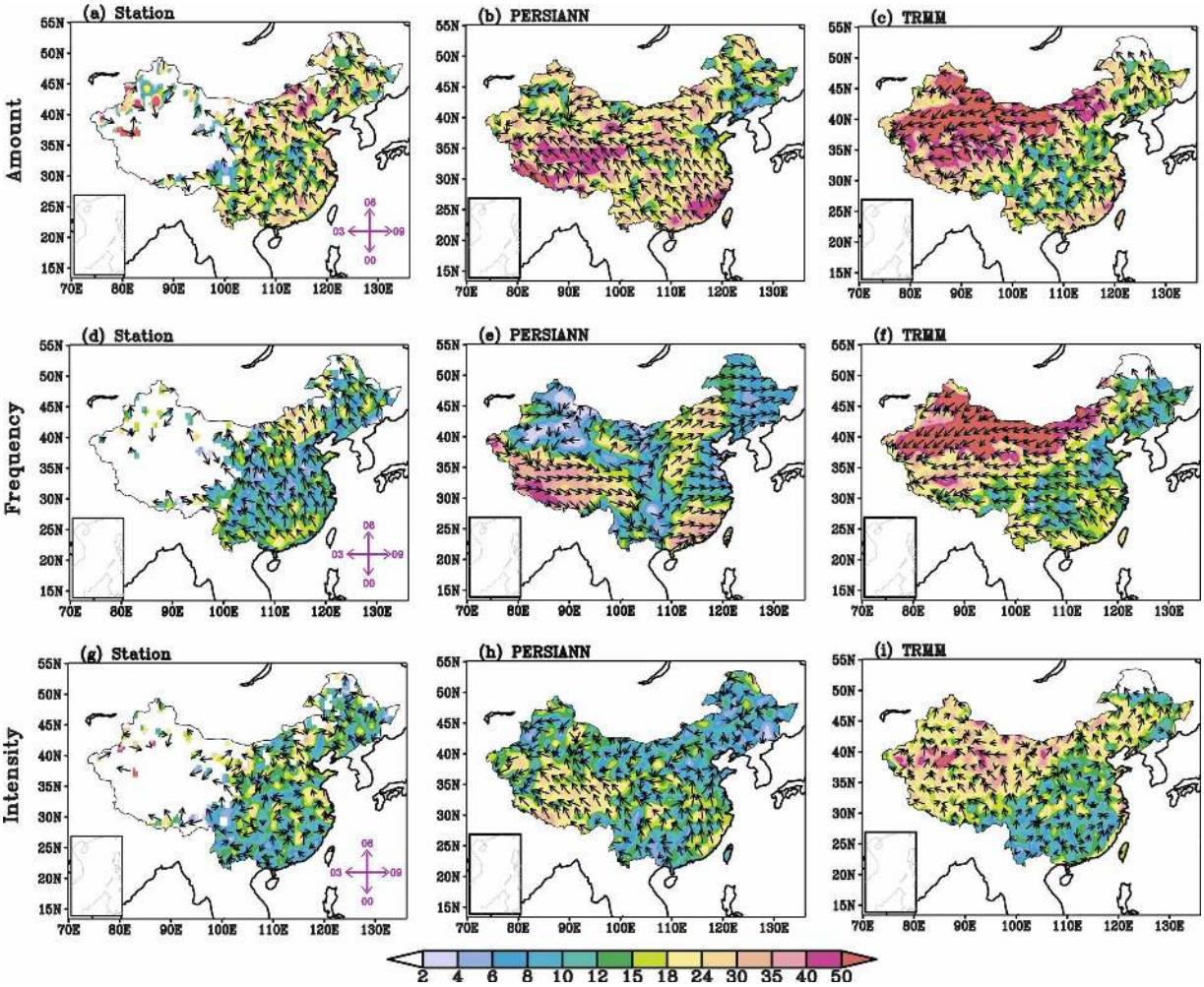

FIG. 7. Same as Fig. 6, but for the 12-h harmonic.

phase also varies eastward along the Yangtze River valley, with a midnight maximum in the upper reaches and a morning maximum in the middle and lower valley. During the spring and fall (i.e., March–May and September–November), the spatial structure of the diurnal phase is relatively noisy, and no coherent large-scale pattern is observed. The midnight maximum over the eastern periphery of the Tibetan Plateau persists throughout four seasons.

5. The mean semidiurnal (12 h) harmonic of precipitation

A previous study of Dai (2001b) found that while the diurnal harmonic dominates the daily variations on most land locations, the semidiurnal harmonic is significant in the oceanic area. Above analyses show that the 24-h cycle predominates over 12 h and shorter time scale variations in most of eastern China. Figure 7 compares the spatial distributions of the amplitudes and phases of the semidiurnal (12 h, S_2) harmonics of the multiyear mean JJA precipitation amount, frequency, and intensity from rain gauges as well as PERSIANN and TRMM products. The 12-h, semidiurnal cycle of precipitation is generally weak over most of eastern China, with amplitudes of less than 15% of the daily mean. Over part of southeastern China and the regions between the Yangtze and Yellow Rivers and northern China, the amplitude of S_2 is larger than 40% in precipitation amount (Figs. 7a–c). A moderate semidiurnal variation is observed over the middle Yangtze River valley. Both the PERSIANN and TRMM products resemble the rain gauges in producing the S_2 amplitude center over southeastern and northern China, but they fail in deriving the center over the regions between the Yangtze and Yellow Rivers. The pattern of S_2 phase is coherent over eastern China, with the time of maximum around 0300 LST in the northern part and 0500

LST in the southern part. A similar phase pattern is seen in frequency maps (Figs. 7d–f). The frequency has a smaller amplitude than the amount does. The pattern of intensity is relatively noisy over eastern China, particular in rain gauge measurements (Figs. 7g–i).

In addition, we have reconstructed the curve of precipitation amount based on the amplitude and phase of a 12-h harmonic for the regional average between the Yangtze and Yellow Rivers. The result indicates that the semidiurnal cycle accounts for 74.2% of the total variance (figure omitted), confirming the result shown in Fig. 3e.

6. Summary and concluding remarks

a. Summary

Characteristics of East Asian summer monsoon precipitation, including spatial patterns in JJA mean precipitation amount, frequency, and intensity as well as the diurnal and semidiurnal cycles, are analyzed by comparing the high-resolution PERSIANN and TRMM products with rain gauge measurements. The focus is the typical summer monsoon domain of eastern China. The comparison provides a reference for the reliability of satellite products over eastern China during 2000–04, and the results should be helpful in evaluating the significance of diurnal variations of precipitation over eastern Asia. The major conclusions are summarized below.

1) The spatial patterns of JJA precipitation amount, frequency, and intensity for PERSIANN and TRMM data are comparable to rain gauge measurements over most of eastern China, as indicated by high pattern correlation coefficients for five subregions ranging from 0.66 to 0.94. The pattern correlation of rainfall amount (0.79 for PERSIANN and 0.94 for TRMM) is higher than that of frequency (0.71 for PERSIANN and 0.77 for TRMM) and intensity (0.66 for PERSIANN and 0.76 for TRMM) over contiguous China. The TRMM product has a better resemblance with rain gauge measurements in terms of both pattern correlation and RMSE value. The frequency (intensity) of satellite products, especially the PERSIANN data, is higher (weaker) than that of rain gauge measurements. The qualities of satellite products are poor over the middle Yangtze River valley in measuring spatial patterns of rainfall frequency and intensity.
2) The diurnal harmonic dominates daily variations of precipitation over most of eastern China. The diurnal variations of summer precipitation amount, frequency, and intensity differ from place to place. A late-afternoon maximum over southeastern and northeastern China and a near-midnight maximum over the eastern periphery of the Tibetan Plateau are seen in rain gauge measurements. The diurnal variation of rainfall amount over eastern China is dominated by both frequency and intensity, as evidenced by both the percentage contribution to the diurnal variance of precipitation amount by frequency and intensity and the relative similarity in the composite diurnal curves for amount, frequency, and intensity, although the contribution of frequency is slightly larger than that of intensity in terms of fractional variance. The diurnal phases of frequency and intensity are similar to that of rainfall amount in most regions.
3) The satellite products overestimate frequency but underestimate intensity of rainfall over eastern China. This is revealed by both the normalized amplitude and daily mean value. The contribution of frequency to the diurnal cycle of rainfall amount is generally overestimated in the satellite products. The nocturnal peak of precipitation amount over the eastern periphery of the Tibetan Plateau and the late-afternoon peak in southern China and northeastern China are captured in both satellite products, except with bias in amplitudes.
4) A robust semidiurnal harmonic for precipitation is seen at the regions between the Yangtze and Yellow Rivers. The diurnal variation of rainfall in this area has two peaks in rain gauge data, with one in the early morning and the other in the late afternoon. The satellite products succeed in measuring the major late-afternoon peak but fail in estimating the secondary early morning peak. The quality of satellite products in the middle Yangtze River valley is also poor.

b. Discussion

Previous studies showed that a stable diurnal cycle may be obtained with just several years of data (Dai et al. 2007). We have compared the results of the 2000–04 mean with those of the 2003–04 mean. While broad features of diurnal variation are the same, some differences were found; for example, the semidiurnal variation over the regions between the Yangtze and Yellow Rivers is different for 2003–04, because the strongest peak appeared in the early morning rather than in the later afternoon as seen in the 2000–04 mean (figure not shown). This indicates an interannual variation of the diurnal cycle.

One interesting feature of the precipitation diurnal cycle over eastern China is the two peaks in the area between the Yangtze and Yellow Rivers. While both

rain gauge and satellite measurements show a major late-afternoon peak, the secondary early morning maximum appears mainly in the rain gauge data but not in the satellite data (Figs. 3–5). The physical processes behind this feature warrants further study. As a beginning for this kind of endeavor, we present a discussion on the possible causes. The late-afternoon maximum can be explained by surface solar heating, which results in maximum low-level atmospheric instability and thus moist convection in the afternoon (Dai et al. 1999; Yu et al. 2007a). The mechanism of the nocturnal or early morning peak is more complex. Lin et al. (2000) mentioned that the nocturnal maximum is a result of stratiform rainfall enhanced by instability due to nocturnal cooling at cloud top. While the nocturnal radiative cooling of clouds might partly contribute to the nocturnal rainfall at the eastern periphery of the Tibetan Plateau due to the existence of an unique continental stratus cloud (Yu et al. 2004; Li et al. 2005), it is not clear whether this can explain the early morning peak observed in the area between the Yangtze and Yellow Rivers. A recent analysis indicates that the early morning peak mainly comes from long-duration rainfall events (i.e., an event that lasts longer than 6 h), while the late-afternoon peak mainly comes from rainfall events lasting less than 3 h (Yu et al. 2007b), implying the importance of stratiform or shallow convections (deep convections) to the early morning (later afternoon) peak. Because the microwave sensing is mainly good for deep convective rainfall (Kummerow et al. 2001), the unsuccessful measurement of the secondary early morning peak in satellite products might be due to the dominance of warm-front cloud or shallow convections over this region. In addition, because this area is partly covered with continental stratus clouds, the low-altitude stratus clouds associated with precipitation are hard to detect with satellites (Yu et al. 2004). The relatively weak diurnal variations over this area also make it harder to detect the secondary peak with satellites.

The diurnal cycle has been serving an observational metric for evaluating model physics. Because the number of rain gauges over China is not enough to provide a complete picture of the rainfall diurnal cycle, satellite products have been regarded as one supplementary data source. Although one motivation for this study is to establish an objective measure for evaluating performances of cumulus parameterizations and other model physics in weather and climate models over eastern Asia and especially China, limitations of satellite products in measuring the diurnal cycle of rainfall over eastern China cast a shadow on this purpose. Nevertheless, the resemblances of satellite products with rain gauge observation in measuring the diurnal cycle over some typical regions, such as the eastern periphery of the Tibetan Plateau and southeastern China, should shed light on the improvements of satellite precipitation algorithms over East Asian monsoon regions.

Acknowledgments. This work was jointly supported by the National Natural Science Foundation of China under Grant Nos. 40523001, 40221503, and 40625014, the National Basic Research Program of China (2006CB403603), and the Chinese Academy of Sciences International Partnership Creative Group, titled "The Climate System Model Development and Application Studies." A. Dai acknowledges the support of NASA Grant No. NNX07AD77G and NCAR's Water Cycle Program. Beneficial discussions with Drs. Yun Qian and Phillip Arkin are highly appreciated. Helpful comments from two anonymous reviewers and the chief editor, Dr. Andrew Weaver, are also gratefully acknowledged.

REFERENCES

Adler, R. F., G. J. Huffman, D. T. Bolvin, S. Curtis, and E. J. Nelkin, 2000: Tropical rainfall distributions determined using TRMM combined with other satellite and rain gauge information. *J. Appl. Meteor.,* **39,** 2007–2023.

Betts, A. K., and C. Jakob, 2002: Study of diurnal cycle of convective precipitation over Amazonia using a single column model. *J. Geophys. Res.,* **107,** 4732, doi:10.1029/2002JD002264.

Bowman, K. P., 2005: Comparison of TRMM precipitation retrievals with rain gauge data from ocean buoys. *J. Climate,* **18,** 178–190.

Chang, K.-T., 2003: *Introduction to Geographic Information Systems* (in Chinese). 2nd ed. Science Press, 245–254.

China Meteorological Administration, 2003: *Specification of Surface Meteorological Observation* (in Chinese). China Meteorological Press, 1–151.

Dai, A., 2001a: Global precipitation and thunderstorm frequencies. Part I: Seasonal and interannual variations. *J. Climate,* **14,** 1092–1111.

——, 2001b: Global precipitation and thunderstorm frequencies. Part II: Diurnal variations. *J. Climate,* **14,** 1112–1128.

——, 2006: Precipitation characteristics in eighteen coupled climate models. *J. Climate,* **19,** 4605–4630.

——, and C. Deser, 1999: Diurnal and semidiurnal variations in global surface wind and divergence fields. *J. Geophys. Res.,* **104,** 31 109–31 125.

——, and K. E. Trenberth, 2004: The diurnal cycle and its depiction in the Community Climate System Model. *J. Climate,* **17,** 930–951.

——, F. Giorgi, and K. E. Trenberth, 1999: Observed and model-simulated diurnal cycles of precipitation over the contiguous United States. *J. Geophys. Res.,* **104,** 6377–6402.

——, X. Lin, and K. Hsu, 2007: The frequency, intensity, and diurnal cycle of precipitation in surface and satellite observations over low- and mid-latitudes. *Climate Dyn.,* **29,** 727–744.

DeMott, C. A., D. A. Randall, and M. Khairoutdinov, 2007: Con-

vective precipitation variability as a tool for general circulation model analysis. *J. Climate,* **20,** 91–112.

Hsu, K.-L., X. Gao, S. Sorooshian, and H. V. Gupta, 1997: Precipitation estimation from remotely sensed information using artificial neural networks. *J. Appl. Meteor.,* **36,** 1176–1190.

——, H. V. Gupta, X. Gao, and S. Sorooshian, 1999: Estimation of physical variables from multichannel remotely sensed imagery using a neural network: Application to rainfall estimation. *Water Resour. Res.,* **35,** 1605–1618.

Huffman, G. J., and Coauthors, 2007: The TRMM Multisatellite Precipitation Analysis (TMPA): Quasi-global, multiyear, combined-sensor precipitation estimates at fine scales. *J. Hydrometeor.,* **8,** 38–55.

Kousky, V., 1980: Diurnal rainfall variation in northeast Brazil. *Mon. Wea. Rev.,* **108,** 488–498.

Kummerow, C., and Coauthors, 2001: The evolution of the Goddard profiling algorithm (GPROF) for rainfall estimation from passive microwave sensors. *J. Appl. Meteor.,* **40,** 1801–1820.

Lee, M.-I., and Coathors, 2007: An analysis of the warm-season diurnal cycle over the continental United States and northern Mexico in general circulation models. *J. Hydrometeor.,* **8,** 344–366.

Li, J., R. Yu, T. Zhou, and B. Wang, 2005: Why is there an early spring cooling shift downstream of the Tibetan Plateau? *J. Climate,* **18,** 4660–4668.

Liang, X.-Z., L. Li, A. Dai, and K. E. Kunkel, 2004: Regional climate model simulation of summer precipitation diurnal cycle over the United States. *Geophys. Res. Lett.,* **31,** L24208, doi:10.1029/2004GL021054.

Lin, X., D. A. Randall, and L. D. Fowler, 2000: Diurnal variability of the hydrologic cycle and radiative fluxes: Comparisons between observations and a GCM. *J. Climate,* **13,** 4159–4179.

Lu, J., 1942: Nocturnal precipitation in Bashan mountain (in Chinese). *Acta Meteor. Sin.,* **16,** 36–53.

Oki, T., and K. Musiake, 1994: Seasonal change of the diurnal cycle of precipitation over Japan and Malaysia. *J. Appl. Meteor.,* **33,** 1445–1463.

Pinker, R. T., Y. Zhao, C. Akoshile, J. Janowiak, and P. Arkin, 2006: Diurnal and seasonal variability of rainfall in the sub-Sahel as seen from observations, satellites and a numerical model. *Geophys. Res. Lett.,* **33,** L07806, doi:10.1029/2005GL025192.

Qian, T., A. Dai, K. E. Trenberth, and K. W. Oleson, 2006: Simulation of global land surface conditions from 1948–2004. Part I: Forcing data and evaluation. *J. Hydrometeor.,* **7,** 953–975.

Shinoda, M., T. Okatani, and M. Saloum, 1999: Diurnal variations of rainfall over Niger in the West Africa Sahel: A comparison between wet and drought years. *Int. J. Climatol.,* **19,** 81–94.

Sorooshian, S., K.-L. Hsu, X. Gao, H. V. Gupta, B. Imam, and D. Braithwaite, 2000: Evaluation of PERSIANN system satellite–based estimates of tropical rainfall. *Bull. Amer. Meteor. Soc.,* **81,** 2035–2046.

Sun, Y., S. Solomon, A. Dai, and R. Portmann, 2006: How often does it rain? *J. Climate,* **19,** 916–934.

——, ——, ——, and ——, 2007: How often will it rain? *J. Climate,* **20,** 4801–4818.

Tao, S., and L. Chen, 1987: A review of recent research on the East Asian summer monsoon in China. *Monsoon Meteorology,* C. P. Chang and T. N. Krishnamurti, Eds., Oxford University Press, 60–92.

Trenberth, K. E., A. Dai, R. M. Rasmussen, and D. B. Parsons, 2003: The changing character of precipitation. *Bull. Amer. Meteor. Soc.,* **84,** 1205–1217.

Wallace, J. M., 1975: Diurnal variations in precipitation and thunderstorm frequency over the conterminous United States. *Mon. Wea. Rev.,* **103,** 406–419.

Yang, G.-Y., and J. Slingo, 2001: The diurnal cycle in the tropics. *Mon. Wea. Rev.,* **129,** 784–801.

Yang, S., and E. A. Smith, 2006: Mechanisms for diurnal variability of global tropical rainfall observed from TRMM. *J. Climate,* **19,** 5190–5226.

Yeh, D. Z., and Y. X. Gao, 1979: *The Meteorology of Qinhai Tibetan Plateau* (in Chinese). Science Press, 211 pp.

Yu, R., B. Wang, and T. Zhou, 2004: Climate effects of the deep continental stratus clouds generated by the Tibetan Plateau. *J. Climate,* **17,** 2702–2713.

——, T. Zhou, A. Xiong, Y. Zhu, and J. Li, 2007a: Diurnal variations of summer precipitation over contiguous China. *Geophys. Res. Lett.,* **34,** L01704, doi:10.1029/2006GL028129.

——, Y. Xu, T. Zhou, and J. Li, 2007b: Relation between rainfall duration and diurnal variation in the warm season precipitation over central eastern China. *Geophys. Res. Lett.,* **34,** L13703, doi:10.1029/2007GL030315.

Zhao, Z., L. R. Leung, and Y. Qian, 2005: Characteristics of diurnal variations of precipitation in China for the recent years. *CLIVAR Exchanges,* No. 3, International CLIVAR Project Office, Southampton, United Kingdom, 24–26.

Zhou, T.-J., and Z. Li, 2002: Simulation of the East Asian summer monsoon by using a variable resolution atmospheric GCM. *Climate Dyn.,* **19,** 167–180.

——, and R.-C. Yu, 2005: Atmospheric water vapor transport associated with typical anomalous summer rainfall patterns in China. *J. Geophys. Res.,* **110,** D08104, doi:10.1029/2004JD005413.